Experimental implementation of a fault handling strategy for electric vehicles with individual-wheel drives

D. Wanner & M. Nybacka
KTH Royal Institute of Technology, Department Aeronautical and Vehicle Engineering, Division of Vehicle Dynamics, Stockholm, Sweden

O. Wallmark
KTH Royal Institute of Technology, Department Electrical Energy Conversion, Stockholm, Sweden

L. Drugge & A. Stensson Trigell
KTH Royal Institute of Technology, Department Aeronautical and Vehicle Engineering, Division of Vehicle Dynamics, Stockholm, Sweden

ABSTRACT: This paper presents a fault handling strategy for electric vehicles with four individual-wheel drives, which are based on wheel hub motors. The control strategy to handle the faults is based on the principle of control allocation and is implemented in an experimental vehicle. Experimental tests has been performed with the experimental vehicle and with simulation. The results show that the directional stability of such a vehicle can be improved for the analysed manoeuvre and failure mode, and the tendencies of the experimental results correspond with the simulation results. It has been found that the lateral and yaw motion could be strongly improved.

Keywords: Vehicle dynamics, fault handling, control allocation, experimental vehicle.

1 INTRODUCTION

The development of new electrified driveline configurations with wheel hub motors (WHM) can reduce the commonly known trade-off between the objectives vehicle handling, comfort and energy efficiency. Vehicles with these types of electrified drivelines are often over-actuated; i.e. more actuators than needed are available to control the degrees of freedom of the vehicle. The implementation of novel control concepts into such over-actuated vehicles enables to switch dynamically between these main objectives depending on the driving situation. Besides the increase of the degrees of freedom on how to control these over-actuated vehicles, it also adds complexity as more components and subsystems are incorporated in this type of vehicles. This is accompanied with an increase of the number of possible faults, which might lead to a change in vehicle behaviour during operation. Further elaboration on these faults can be found in the comprehensive study performed in previous studies by the author, where both analysis and classification of faults has been conducted (Wanner et al. 2014). Here, a method for the classification of faults according to their influence on the dynamic behaviour of a vehicle is also proposed. A failure can influence the vehicle behaviour to such a degree that a fatal accident could occur and the anti-lock braking (ABS) or electric stability control (ESC) might not be enough to manage this fault (Wanner et al. 2015). This is why it is important to study the severity of faults and how over-actuated vehicles can be controlled in case of a fault to mitigate the effect the fault have on the vehicle behaviour. Various studies have been analysing the influence of faults on the dynamic behaviour of a vehicle, e.g. (Jonasson et al. 2008), (Li et al. 2014) and (Park et al. 2012).

In this work, a fault handling strategy is presented and analysed for one possible failure mode in an over-actuated electric experimental vehicle, the KTH Research Concept Vehicle (RCV). In section 2, the control architecture and the chosen control method is described, which is based on

the control allocation principle. The RCV and its electric driveline, which incorporates a wheel hub motor in each of the four wheels, is presented in section 3. Results are presented in section 4. The paper is finalised with concluding remarks in section 5.

2 CONTROL ARCHITECTURE

A closed-loop control architecture is proposed as fault-tolerant control system. Vehicle velocities and the information about an active fault are the states that are fed back to the controller. The input to the control system is determined by a driver interpreter. This driver interpreter transforms the driver input signals, accelerator pedal position, ϵ, and steering wheel angle, δ_{sw}, into reference longitudinal and lateral velocity, v_x^{ref} and v_y^{ref}, and the reference yaw rate, $\dot{\psi}^{\text{ref}}$. These input signals are used in a control system that is implemented in a simulation model and in an experimental vehicle.

The output of the driver interpreter as well as the feedback states are fed into the dynamic motion controller. This PI-controller compares the desired reference vehicle velocities (v_x^{ref}, v_y^{ref}, $\dot{\psi}^{\text{ref}}$) with the measured vehicle velocities (v_x, v_y, $\dot{\psi}$) in order to minimise the tracking error and calculate the desired longitudinal and lateral reference vehicle force and the yaw torque acting on the vehicle's center of gravity (F_x^{ref}, F_y^{ref}, M_z^{ref}). In addition, a cruise control function with an speed-dependent anti-windup scheme was integrated in the dynamic motion controller.

In the control allocator, the reference vehicle forces and the yaw torque are processed according to the principle of control allocation (CA) in order to follow a desired trajectory. As the number of controlled actuators is higher than the number of degrees of freedom, CA is a mathematically under-determined problem which leads to an infinite amount of solutions. It can be solved with help of the pseudo-inverse control allocation strategy (PCA), which requires a low computational effort and run time (Oppenheimer et al. 2006). This approach applies a rule-based mathematical alternative solution based on the Moore-Penrose pseudoinverse (Bodson 2002) for finding the inverse of a non-quadratic matrix without optimisation. Limiting factors of this strategy are the actuator and dynamic tyre force constraints, which are not taken into consideration by the pseudo-inverse algorithm. In the analysed vehicle at-hand, the over-actuation is limited to the four wheel hub motors while a normal front wheel steering system is used. As only longitudinal actuators are controlled in this study, the vehicle forces and yaw torque are reduced to the longitudinal vehicle force F_x^{ref} and vehicle yaw torque M_z^{ref}, which are distributed to the longitudinal tyre forces ($f_{x1}'^{\text{ref}}$, $f_{x2}'^{\text{ref}}$, $f_{x3}'^{\text{ref}}$, $f_{x4}'^{\text{ref}}$) in each wheel hub motor. The lateral vehicle force F_y^{ref} is assumed to be small and therefore not considered.

The general relation between the vehicle forces and torques and the directional forces is adjusted to $\mathbf{F}^{\text{ref}} = [F_x^{\text{ref}}\ M_z^{\text{ref}}\ 0\ ]^T$. An additional row for fault identification is introduced and the lateral vehicle force is removed. This relation between vehicle forces and yaw torque and the directional forces is given as

$$\mathbf{F}^{\text{ref}} = \mathbf{B}'\mathbf{f}_x'^{\text{ref}} \tag{1}$$

with the longitudinal tyre force matrix

$$\mathbf{B}' = \begin{bmatrix} \cos\delta_1 & -0.5s\cos\delta_1 + l_f\sin\delta_1 & k_{f,1} \\ \cos\delta_2 & 0.5s\cos\delta_2 + l_f\sin\delta_2 & k_{f,2} \\ 1 & -0.5s & k_{f,3} \\ 1 & 0.5s & k_{f,4} \end{bmatrix}^T .$$

The introduced additional column for fault identification is coupled to the feedback of the fault detection and isolation (FDI) and allows the allocation of longitudinal forces to the remaining healthy WHMs that are not affected by the fault. The FDI signals define the location of healthy and faulty wheels according to equation (2) and changes the longitudinal tyre matrix $\mathbf{B}'$ dynamically.

$$k_{f,i} = \begin{cases} 0 & \text{healthy wheel} \\ 1 & \text{faulty wheel} \end{cases} \tag{2}$$

After solving equation (1) for $\mathbf{f}_x'^{\text{ref}}$, the reference WHM torques are governed by

$$\mathbf{M}'^{\text{ref}} = r\mathbf{B}'^{\dagger}\mathbf{F}^{\text{ref}}, \tag{3}$$

where the pseudoinverse $\mathbf{B}'^{\dagger}$ of the non-invertible matrix $\mathbf{B}'$ is derived as

$$\mathbf{B}'^{\dagger} = \mathbf{B}'^{T}(\mathbf{B}'\mathbf{B}'^{T})^{-1}.$$

A drawback of SCA is that propulsion torques are allocated to the wheels even when tyre force or actuator constraints are exceeded. Furthermore, the allocation is independent of normal loads, i.e. friction utilisation among the tyres can vary a lot during longitudinal and lateral load transfer.

The fault detection and isolation function has been emulated in the control structure by providing a feedback of the WHM fault state instantly after its occurrence. With this information, the faulty actuator can be isolated and the control allocator can be re-configured by distributing the reference vehicle forces and yaw torque onto the three available actuators.

The presented control architecture has previously been developed and is described in detail in (Wanner, 2015).

3 EXPERIMENTAL VEHICLE

The RCV is an experimental vehicle platform for effectively validating and demonstrating research aiming towards finding sustainable transport solutions of the future. It is a pure electric vehicle where each wheel corner module is equipped with a wheel hub motor and individual steering and camber actuators. This high level of over-actuation allows a broad range of experimental evaluation in the fields of vehicle dynamics, mechatronics, control theory, electro mechanics, etc. The RCV is displayed in Figure 1.

The electric driveline consists of four identical wheel corner modules, which is based on the patented autonomous corner module concept (Zetterström 2002 and 2004). Each wheel corner module can be propelled, braked, steered and cambered individually and is equipped with a 36 pole, 2 kW PRA-230 wheel hub motor of permanent-magnet synchronous type, capable of developing 150 Nm during a short interval. Each motor is fed by a Kollmorgen ACD 4805 converter which, in turn, is supplied from an in-house designed 52V/40Ah lithium-ion battery pack. At a rated load of 33 Nm and 520 rpm, the measured efficiency of the converter is 94.4 %. By connecting two motors back-to-back and measuring the input and output power, the efficiency at the rated load for one motor is estimated to 85.6 % (Silva, 2013). More detail on the RCV including its other subsystems is found in (Wallmark et al. 2014).

All actuators of the RCV are controlled by using a dSPACE MicroAutoBox coupled to a graphical user interface. The control architecture is modular, which enables an easy exchange of individual controller blocks for testing purposes. In the standard configuration, which is also used as a basis to compare to, the controller is set to four wheel drive with front wheel steering, where the traction torque request from the accelerator pedal is equally distributed to the four wheel hub motors. The previously presented CA strategy has then been implemented in the RCV.

4 RESULTS

The described control architecture has been analysed in experiments with the RCV. The driven manoeuvre was a straight line driving manoeuvre at a speed of 9 m/s. The implemented failure was a strong brake torque on the left rear wheel, which was implemented with the previously mentioned auxiliary brake system. When the failure was triggered, the pressure was quickly increased up to 50 bar until the rear left wheel locked and held for approximately 2 s before it was released again. The manoeuvre was once driven with the control allocation strategy (PCA) and once with no vehicle control (NVC). The steering wheel angle as well as the accelerator and brake pedal positions were electronically set to a constant value during the failure was active. The results of the vehicle without (marked in red) and with (marked in blue) implemented fault handling strategy are displayed in Figures 2–5.

In Figure 2, the vehicle position is displayed for both cases, PCA and NVC. The black dashed line indicates the healthy vehicle trajectory. The failure was triggered at position $(x, y) = (0, 0)$ m

Figure 1. The KTH Research Concept Vehicle 2014.

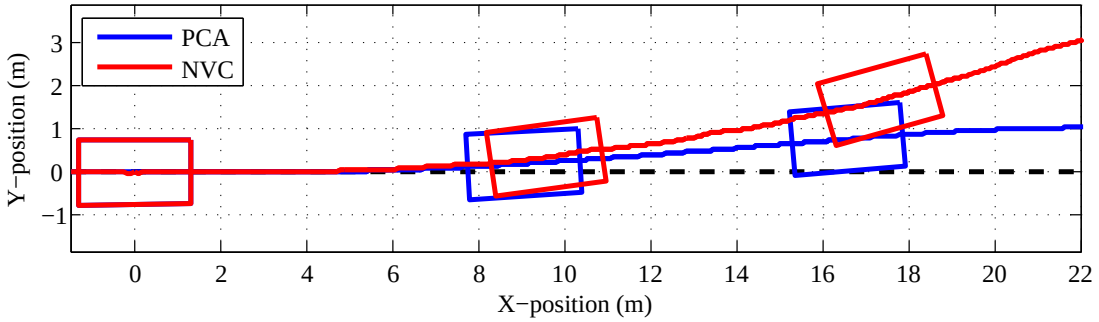

Figure 2. X-Y-positions for the vehicle with and without CA during failure activation at 9 m/s starting at X = 0 m. The black dashed line is the path without failure.

with the auxiliary brake system. The experimental vehicle deviated from its intended trajectory for the controlled and the uncontrolled vehicle after the failure was triggered. It can be seen that the manoeuvre with NVC has a clear lateral deviation from the straight path of 3 m after 22 m. The PCA strategy has a lateral deviation of 1 m at the same longitudinal position. The latter lateral deviation is due to the actuator limitations of 150 Nm on each of the wheel hub motors.

The vehicle states longitudinal speed and yaw rate of both cases are shown in Figure 3. At 2 s after failure activation, a speed reduction of $v_x = 2.45\,\text{m/s}^2$ is seen for PCA and NVC. The yaw rate of the uncontrolled vehicle had a constant yaw rate of 8 deg/s, while the controlled vehicle reached a lower values (blue dashed line). Hereby, the maximum yaw rate increased during the first second to 6.42 °/s before it dropped again to the reference yaw rate after 1.7 s.

Despite the same speed reduction, the differences in maximum absolute longitudinal accelerations $|a_{x,max}|$ differed with 2.19 m/s^2 and 2.48 m/s^2 from one another as seen in Figure 4. The lateral acceleration distinguished accordingly. The vehicle with the PCA strategy had a slower build up in lateral acceleration and reached its minimum value at -0.87 m/s^2 within the first second after failure induction. Afterwards, lateral acceleration reduced to almost zero.

The torque distribution to each of the wheels is seen in Figure 5. On the left, the allocated reference torques are displayed. When the failure is activated at 0 s, the reference torque of the left front wheel is increasing in order to compensate for the braking torque on the left rear wheel. The latter is additionally set to zero as long as the failure was activated. Both reference torques to the wheels on the right side of the vehicle were allocated in the same way. The change in the torque characteristics at 0.8 s is due to the cruise control function. Thereby, the priorities of the deviations in longitudinal and yaw motion are switched after a certain threshold. The wheel torques on the right front and rear wheel were reduced to achieve a yaw compensation. On the

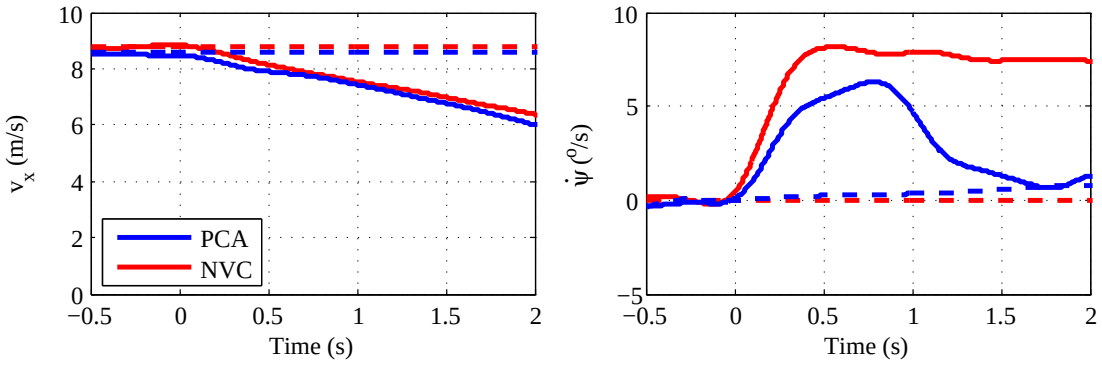

Figure 3. Longitudinal speed and yaw rate for the vehicle with and without CA during failure activation at 9 m/s starting at t = 0 s. The dashed red and blue lines are the desired reference states.

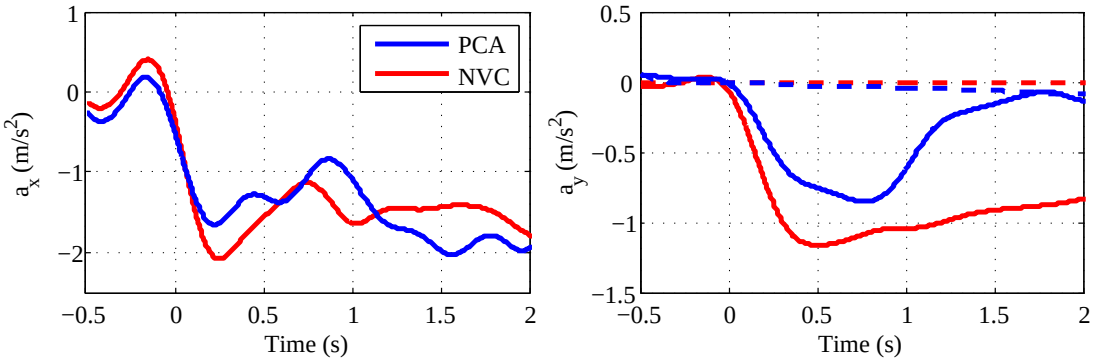

Figure 4. Longitudinal and lateral acceleration for the vehicle with and without CA during failure activation at 9 m/s starting at t = 0 s. The dashed red and blue lines are the desired reference states.

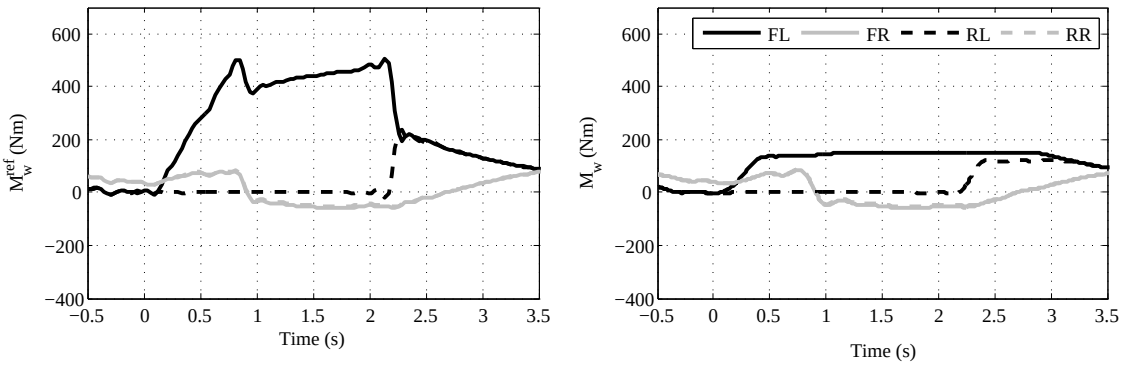

Figure 5. Reference and actual wheel torques during failure condition starting at t = 0 s.

right side of Figure 5, the actual torques are shown. All torques represent the allocated reference torques, except for the torque on the left front wheel. Here, the actuator was limiting the torque allocation to the maximum possible torque of the WHM. The actual wheel torques of NVC were kept constant during the failure condition on all three healthy wheels.

The results were further analysed with the evaluation criteria of the fault classification method that was developed and tested in (Wanner et al. 2014). Thereby, three evaluation criteria analysed longitudinal, lateral and yaw motion during the first time period after failure induction. The first criterion was the collision avoidance index Q_x, which slightly improved for PCA compared to NVC due to the actuator limitations. The second criterion was the lane keeping index Q_y. Here, a strong improvement of more than 50 % has been achieved with PCA. The vehicle stability

Table 1. Analysed evaluation criteria and their comparison for PCA and NVC.

Parameter	NVC	SCA	Change
Q_x (m/s^2)	-2.79	-2.10	-24.6
Q_y (t)	1.61	2.49	+54.7
Q_z ($^\circ$/s^2)	14.92	7.16	-52.0

index Q_z represents the third criterion, which also reduced by half when PCA was active during the failure. The three evaluation criteria confirmed that the experimental study without driver in the loop showed a clear improvement of the vehicle behaviour when applying the PCA strategy. Detailed explanation and definitions of the criteria can be found in (Wanner et al. 2014). In Table 1, the resulting values of the three criteria are summarised and compared.

5 CONCLUSIONS

The presented fault handling strategy has been implemented in an experimental vehicle. The results of the driven manoeuvre showed that the activated failure could be handled well by the pseudo-inverse control allocation strategy. This was a strong improvement compared to the uncontrolled vehicle. The yaw rate was reduced significantly despite the actuator limitations of the wheel hub motors of the RCV. The lateral acceleration was reduced to a similar extend, while the speed kept on the same level for both cases due to the mentioned actuator limitations. An evaluation based on the previously developed fault classification method confirmed these findings. The lane keeping index as well as the vehicle stability index for PCA improved by more than 50 % compared to NVC. It has been shown that this fault handling strategy can be a possible control method in case of a fault for electric vehicles with wheel hub motors.

REFERENCES

Bodson, M. 2002. Evaluation of optimization methods for control allocation, *J. Guidance, Control, and Dynamics*, vol. 25, no. 4, pp. 703–711.

M. Jonasson and O. Wallmark, *Control of electric vehicles with autonomous corner modules: implementation aspects and fault handling*, J. Vehicle Systems Modeling and Testing, vol. 8, no. 3, pp. 213–228, 2008.

Li, C., Chen, G. and Zong, C. *Fault-tolerant control for 4WID/4WIS electric vehicles*, presented at SAE World Congr. Exhibit., 2014, Tech. Paper 2014-01-2589.

Oppenheimer, M.W., Doman, D.B. and Bolender, M.A. 2006. Control allocation for over-actuated systems. In *IEEE Control and Automation; Proc. Mediterranean Conf.*, Ancona, Italy.

Park, G., Son, B., Kum, D., Lee S. and Kwak, S. *Dynamic modeling and simulation for battery electric vehicles under inverter fault conditions*, J. Applied Mechanics and Materials, vols. 110-116, pp. 3007–3015, 2012.

Silva, L.C. 2013. *Modeling and design of the electric drivetrain for the 2013 Research Concept Vehicle*. Master thesis, KTH Royal Institute of Technology, Stockholm, Sweden, XR-EE-E2C 2013:008.

Wallmark, O., Nybacka, M., Malmquist, D., Burman, M., Wennhage, P. and Georén, P. 2014. Design and implementation of an experimental research and concept demonstration vehicle. In *IEEE Vehicle Power and Propulsion Conf.; Proc.*, Coimbra, Portugal.

Wanner, D., Drugge, L. and Stensson Trigell, A. 2014. Fault classification method for the driving safety of electrified vehicles, *J. Vehicle System Dynamics*, vol. 52, no. 5, pp. 704-732.

Wanner, D., Wallmark, O., Jonasson, M., Drugge, L. and Stensson Trigell, A. 2015. Control allocation strategies for an electric vehicle with a wheel hub motor failure, *Int. J. Vehicle Systems Modelling and Testing*, in press.

Zetterström, S. 2002. Electromechanical steering, suspension, drive and brake modules. In *56th IEEE Vehicular Technology; Proc. Conf.*, Vancouver, Canada.

Zetterström, S. 2004. *Wheel suspension arrangement in a vehicle*. Patent EP 1 144 212, date granted: 07.07.2004.